Non-destructive dose verification of two drugs within 3D printed polyprintlets

Sarah J Trenfield[1], Hui Xian Tan[1], Alvaro Goyanes[2], David Wilsdon[3], Martin Rowland[4], Simon Gaisford[1,2] and Abdul W Basit[1,2]*

[1]UCL School of Pharmacy, University College London, 29-39 Brunswick Square, London WC1N 1AX, UK

[2]FabRx Ltd., 3 Romney Road, Ashford, Kent, TN24 0RW, UK

[3]Pfizer Ltd., Analytical Research and Development, Discovery Park, Ramsgate Road, Sandwich, CT13 9ND, UK

[4]Pfizer Ltd., Drug Product Design, Discovery Park, Ramsgate Road, Sandwich, CT13 9ND, UK

*Correspondence: a.basit@ucl.ac.uk (Abdul W. Basit)

Key words: 3D printing; Selective laser sintering; Process analytical technology (PAT); Oral drug delivery systems; Near infrared spectroscopy; Digital healthcare; Personalized medicines

Abstract

Three-dimensional printing (3DP) is a revolutionary technology in pharmaceuticals, enabling the personalisation of flexible-dose drug products and 3D printed polypills (polyprintlets). A major barrier to entry of this technology is the lack of non-destructive quality control methods capable of verifying the dosage of multiple drugs in polyprintlets at the point of dispensing. In the present study, 3D printed films and cylindrical polyprintlets were loaded with flexible, therapeutic dosages of two distinct drugs (amlodipine and lisinopril) across concentration ranges of 1-5% *w/w* and 2-10% *w/w*, respectively. The polyprintlets were non-destructively analysed for dose content using a portable near infrared (NIR) spectrometer and validated calibration models were developed using partial least squares (PLS) regression, which showed excellent linearity (R^2 Pred = 0.997, 0.991), accuracy (RMSEP= 0.24%, 0.24%) and specificity (LV1= 82.77%, 79.55%) for amlodipine and lisinopril, respectively. X-ray powder diffraction (XRPD) and thermogravimetric analysis (TGA) showed that sintering partially transformed the phase of both drugs from the crystalline to amorphous forms. For the first time, we report a non-destructive, RTR quality control of two separate active ingredients in a single 3D printed drug product using NIR spectroscopy, overcoming a major barrier to the integration of 3D printing into clinical practice.

1. Introduction

Hypertension is a silent killer, responsible for over 7.5 million deaths / year (12.8% of all deaths) worldwide (WHO, 2019). Polypharmacy, which signifies the concurrent use of multiple medications by one individual, is the current gold standard for treating hypertension (Durden et al., 2013) (NICE, 2011). Due to polypharmacy, medication adherence is a major challenge in the management of hypertension, with over 65% of patients failing to adhere to their prescribed regimens, and 50% ceasing their medication regime within one year of prescription (Ruilope, 2011; Tibebu et al., 2017) (Abegaz et al., 2017; Corrêa et al., 2016).

Critically, a long-term non-adherence to treatment has been associated with an increased risk of cardiovascular events, including strokes, hospitalisations and death (Abegaz et al., 2017; Herttua et al., 2013; Lee et al., 2017; Ong et al., 2007). To resolves the issues arising from polypharmacy, the use of fixed drug combinations (also known as ‘polypills’) have been explored. However, although polypills have been shown to improve adherence, the dosage of each drug is fixed making changes in dosage regimens inconvenient (Roy et al., 2017). In order to overcome this, there is a need for a novel platform that enables flexible dosing for polypills and three-dimensional printing (3DP) has the potential to do so (Alomari et al., 2018; Trenfield et al., 2019a).

3DP has gained momentum in many industries such as the aeronautics, robotics, electronics, manufacturing and food industries and, more recently, within medicine and pharmaceuticals (Barnatt, 2013). Within the pharmaceutical field, it is no longer a new idea to transition away from the standard mass production of medicines of fixed strength towards creating personalised dosage forms and dose combinations (Awad et al., 2018a; Awad et al., 2018b; Goyanes et al., 2017). By creating medicines in a layer-by-layer manner, this technology can produce printlets (3D printed tablets) that are customised to a patient’s disease state, individual factors and therapeutic needs (Florence and Lee, 2011; Goyanes et al., 2019b; Hamburg and Collins, 2010; Oblom et al., 2019; Trenfield et al., 2018a). Due to the ability for precise

material deposition, several studies have demonstrated the potential for 3DP to create polypills (polyprintlets) containing more than one active pharmaceutical ingredient (API) (Genina et al., 2017; Gioumouxouzis et al., 2018; Khaled et al., 2015a, b; Robles-Martinez et al., 2019; Sadia et al., 2018b).

Whilst the evidence-based for 3DP of polyprintlets is increasing, the integration of this technology into clinical practice has not yet been achieved (Alhnan et al., 2016; Basit and Gaisford, 2018; Edinger et al., 2018). A major barrier preventing 3DP uptake into pharmaceuticals is the absence of an at-line, non-destructive quality control (QC) techniques to enable the real-time release of 3D printed medicines (Di Prima et al., 2016; Trenfield et al., 2018b; Trenfield et al., 2019b). Analytical methods such as dose quantification using chromatographic methods, as well as dissolution and disintegration testing, are commonly used for QC of pharmaceuticals. However, these characterisation methods are inherently destructive, which would be inconvenient for individually fabricated printlets at the point-of-care (Awad et al., 2018a).

An alternative approach could involve the integration of real-time release (RTR) testing, which is the ability to evaluate and ensure the quality of in-process and/or final product based on process data (EMA, 2012). Vibrational spectroscopic tools, such as near infrared (NIR) spectroscopy combined with chemometrics, have previously been used as alternative QC tools within pharmaceutical processes (Edinger et al., 2019; Trenfield et al., 2018b; Vakili et al., 2017). NIR spectroscopy has been widely used for at-line analysis because it has the capability to analyse and quantify drugs in a rapid, non-destructive and user-friendly manner. Furthermore, it can be conveniently integrated at the point of dispensing in the clinic due to its portability. The potential for NIR spectroscopy as a non-destructive QC method was demonstrated by our group previously whereby a point-and-shoot approach was used to measure the drug content of paracetamol in printlets (Trenfield et al., 2018b).

To date, previous research had predominantly focused on quantifying single active ingredients within individually fabricated dosage forms using NIR

spectroscopy (Trenfield et al., 2018b). However, one of the major benefits of 3DP is the ability to produce polyprintlets containing multiple APIs in the same dosage form (Pereira et al., 2018; Xu et al., 2020). As such, for the first time, we demonstrate the non-destructive QC of two distinct APIs (lisinopril and amlodipine) at therapeutically-relevant dosages within 3D printed polyprintlets using a portable, reflectance NIR spectrometer. The applicability of the model to polyprintlets of different geometries (cylindrical and oral films) was evaluated, and dosage forms were characterised using x-ray powder diffraction (XRPD) and thermogravimetric analysis (TGA) to elucidate drug distribution and solid-state characteristics.

2. Materials and Methods

Amlodipine (LKT Laboratories, Inc., US) (MW 408.879 g/mol, solubility at 25°C 75.3 mg/L) (Pubchem, 2003) and lisinopril dihydrate (Acros Organics, UK) (MW 441.525 g/mol, solubility at 25°C 216 mg/L) (DrugBank; Pubchem, 2005). Polyethylene oxide (PEO) 100,000 (Sigma-Aldrich, UK) which has a molecular weight of 100,000 g/mol and density of 1.13 g/mL (Pubchem, 2004) was used as the thermoplastic polymer in the sintering process. Candurin ® Gold Sheen was purchased from Merck KGaA, Germany.

2.1. 3D printed design

Templates of the printlets were designed by using 123D Design Software (Autodesk Inc, UK), a computer-aided design (CAD) software to create 3D representations of the object. Oral square films (10 mm x 10 mm x 0.5 mm) and standard cylindrical printlets (10 mm diameter x 3.6 mm height) were designed. 3D models were exported as a stereolithographic (.stl) file into 3D printer Sintratec Central software Version 1.1.13.

2.2. Printing process

PEO 100,000 was sieved by using a 180 µm orifice-size sieve to reduce its particle size for printing. Twenty-five formulations were prepared for building the calibration model for NIR spectroscopy across five different dosage concentration ranges (n = 5, Table 1). The lowest and highest concentrations of both drugs were selected to enable the provision of therapeutically-relevant dosages, i.e. assuming a 200mg tablet is produced, amlodipine 1-5%w/w covers a 2mg – 10mg dose range and lisinopril 2-10%w/w covers a 4mg – 20mg dose range. For each formulation, 15g of a mixture of drugs and excipients were blended using a pestle and mortar. 3% *w/w* of Candurin Gold Sheen was added to all formulations to enhance absorption of the laser to allow printability (Fina et al., 2017). The powder mixtures were transferred to a selective laser sinter (SLS) printer (Sintratec Kit, AG, Brugg, Switzerland) for printing. The chamber temperature (which indicates the temperature inside the printer body) was maintained at 30 °C and the surface temperature (which refers to the temperature of the powder bed surface in the build platform) was maintained at 40 °C. The laser scanning speed was set at 200 mm/s. The printing process started with the activation of a 2.3 W blue diode laser (445 nm) to sinter the powder within the build platform in a certain pattern based on the .stl file. Powder in the reservoir platform (150 mm x 150 mm x 30 mm) of the printer was moved by a sledge to a building platform (150 mm x 150 mm x 30 mm) creating a flat and homogeneously distributed layer of powder. Then, the laser would sinter on the powder particles together. This process was repeated layer-by-layer until the object was completed. The dosage form was then removed from the powder bed and excess powder was brushed off. Five oral films were printed at the same time for each formulation. Three formulations (A2L4, A3L6 and A4L8) were chosen to be printed into cylindrical tablets for inclusion into the building the calibration model (n=3).

Table 1. Formulation composition for calibration model printing

Formulation code	Drug concentration (% *w/w*)		PEO (% *w/w*)	Candurin Gold Sheen (% *w/w*)
	Amlodipine	Lisinopril		
A1L2	1	2	94	3
A2L4	2	4	91	3
A3L6	3	6	88	3
A4L8	4	8	85	3
A5L10	5	10	82	3

2.3. Near infrared spectroscopy (NIR) data acquisition

A portable benchtop Labspec 5000 NIR spectrometer (Analytical Spectral Devices, USA), equipped with three separate holographic diffraction gratings and three separate detectors; a 512-element silicon photo-diode array for wavelengths between 350–1000 nm, and two TE-cooled InGaAs for wavelengths between 1000–1800 nm and 1800–2500 nm was used to measure the NIR reflectance. An immobilised lab grade 1 m fibre optic cable (fibre core size 200 µm), which interfaced with the NIR equipment (BIF200- Vis-NIR, Ocean Optics Inc., FL, USA) was used to collect the spectra. A Spectralon 99% reflective standard (Labsphere, North Sutton, UK) was used for instrument calibration prior to spectra acquisition. UV–visible-NIR spectra were collected across the 350–2500 nm wavelength region (2150 data points) totalling 64 scans, which were averaged. Each printlet was analysed at six different points to avoid potential sampling errors and to reduce the variability caused by different surface effects. All printlets were scanned three times on each side with the same format. The final spectrum (used to calculate amlodipine and lisinopril content) was the average of the spectra recorded at the six positions (6 averaged spectra/tablet). The data was processed by using Microsoft Excel and MATLAB software version R2017a (The MathWorks, CA, USA).

2.4. Model development

All five oral film concentrations (n=5) (amlodipine 1-5% *w/w*; lisinopril 2-10% *w/w*; Table 1) were selected for calibration model development. Two oral films from A2L4, A3L6 and A4L8 was used for internal validation. Multivariate data analysis was performed using MATLAB software version R2017a (The

MathWorks, CA, USA) with the PLS Toolbox version 8.6 (Eigenvector, CA, USA) for data pre-processing and modelling. Partial least squares (PLS) regression was performed on the datasets to build calibration models. The models were internally cross-validated using Venetian blinds. Validation of the NIR calibration model was performed according to guidance from the International Conference on Harmonization (ICH) guidance Q2(R1)(ICH, 1994b)), European Medicines Agency (EMA) (EMA, 2014b) and the Food and Drug Administration (FDA) (FDA, 2015a), by assessing model specificity, linearity (expressed as correlation coefficient, R^2) and accuracy (expressed as the root mean square error of prediction; RMSEP). The calibration model developed covered a total of 25 samples of oral films (with 19 samples being selected for calibration and 6 samples for internal validation) over an amlodipine concentration range of 1-5% *w/w* and lisinopril concentration range of 2-10% *w/w*.

2.5. Determination of drug content

Three individual oral film printlets of each formulation were placed in separate volumetric flasks with deionised water and methanol (50:50). Samples of the solution were then filtered using a 0.45 µm membrane filter (Millipore Ltd., Ireland) into the HPLC vials. HPLC analysis was performed using UV-HPLC equipped with an Eclipse Plus C18 column (150 x 4.6 mm, 5 µm particle size) (Agilent, UK) at a temperature of 40℃. Analyses were carried at a detection wavelength of 215 nm, a flow rate of 1 mL/min, an injection volume of 100 µL and a run time of 18 mins. The mobile phase consisted of a gradient of solvent A (HPLC water adjusted to pH 3 with phosphoric acid) and solvent B (acetonitrile). The method entailed the following: 1) solvent A and solvent B were set at 83:17 at the start time; 2) then adjusted to 80:20 at the 6^{th} minute; 3) then adjusted to 10:90 at the 15^{th} minute 4) adjusted to 83:17 at the 18^{th} minute. Elution times for amlodipine and lisinopril were 1.9 mins and 11.1 mins, respectively.

2.6. X-ray powder diffraction

A Rigaku MiniFlex 600 (Rigaku, USA) with a Cu Kα X-ray source (λ = 1.5418 Å) and accompanying software Miniflex Guidance version 1.2.01 were used to

record x-ray powder diffraction (XRPD) patterns of printlets (ground to fine powder), formulation blends and pure amlodipine, lisinopril, PEO 100,000 and Candurin Gold. The intensity and voltage applied were 15 mA and 40 kV respectively. The angular range of data acquisition was 3–40° 2θ, with a step size of 0.02° at a speed of 2° min^{-1}.

2.7. Thermal analysis

Thermogravimetric analysis (TGA) was also used for characterisation. All the samples were heated at 10 °C min until 400 °C in open aluminium pans using Discovery TGA (TA instruments, Waters, LLC, USA). The purge gas used was nitrogen gas with a flow rate of 25 mL/ min. Data were collected and analysed by using TA Instruments Trios software and percentage mass loss and onset temperature were calculated. The results from thermal analysis were plotted using OriginPro Software (OriginPro 2017 (64 bit) SR2 b9.4.2.380).

2.8. Characterisation of the printlets

2.8.1. Determination of printlet weight variability

All cylindrical printlets were weighed by using a weighing balance (Sartorius AG CPA225D, Germany). Printlets were measured in triplicate, and the mean and standard deviation for each printlet was calculated.

2.8.2. Determination of printlet strength

A traditional tablet hardness tester TBH 200 (Erweka GmbH, Heusenstamm, Germany) was used to determine the crushing strength of three cylindrical printlets of each drug combination. The mean and standard deviation for each printlet was calculated.

2.8.3. Determination of printlet friability

Three tablets of each concentration were weighed and placed into the drum of a Friability Tester Erweka type TAR 10 (Erweka GmbH, Heusenstamm,

Germany). The drum was rotated at 25 rpm for 100 rounds and the samples were reweighed. The friability of these samples was analysed in terms of weight loss and it was expressed as percentage of original sample weight.

3. Results and Discussion

For the first time, it was possible to use a low temperature SLS printing process to manufacture 3D printed oral square films and cylindrical printlets containing two drugs (amlodipine and lisinopril) at therapeutically relevant concentrations (up to 5% *w/w* and 10% *w/w,* respectively; Figure 1). Previously studies have proven the feasibility of using SLS 3DP technology in the pharmaceutical field by successfully manufacturing immediate and modified release tablets (Barakh Ali et al., 2019; Fina et al., 2017; Fina et al., 2018a), as well as fast disintegrating oro-dispersible tablets (Fina et al., 2018b). Awad *et al*. has also shown the capability of SLS 3D printing to produce pellets (miniprintlets) containing more than one drug (Awad et al., 2019). However, the majority of these studies required the use of elevated temperatures (80 – 135 °C) to enable effective sintering. Favourably, due to low T_g of the polymer (PEO 100,000, T_g of -67 °C), it was possible to manufacture the dosage forms at a low temperature (40 °C), which could be highly beneficial for thermally-labile drugs that are unsuitable for higher temperature 3D printing processes (Goyanes et al., 2015a).

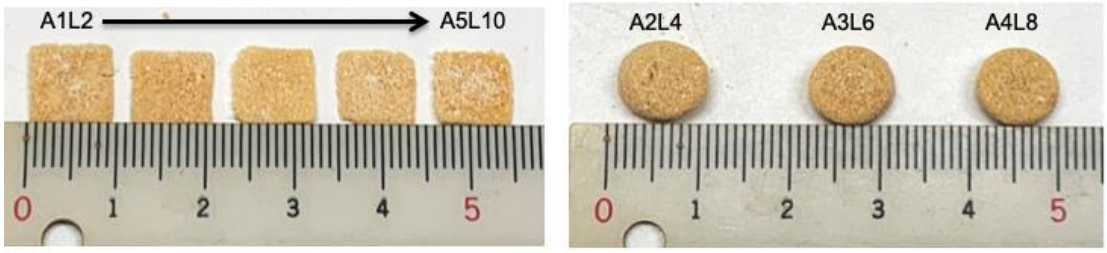

Figure 1. Printlets of two different geometries; square oral film (left) and cylindrical shape tablet (right). Drug content increases from left to right. The scale is in cm.

3.1. Polyprintlet characterisation

Initially, TGA was performed to evaluate whether the drugs would be stable at the temperatures required during the sintering process (Figure 2). The results

showed that lisinopril decomposition occurred gradually in three steps. A weight loss of ~8% was observed up to 100°C, attributed to the loss of water due to lisinopril being in the dihydrate form. A constant weight was maintained between 100-175℃ indicated that no alteration occurred in the dehydrated lisinopril crystal during this stage. Beyond 175℃, the lisinopril crystal melted (T_m = 178-179℃) and degraded, which is similar to findings reported in the literature (Hinojosa-Torres et al., 2008). TGA data of the other components (amlodipine and PEO 100,000) and the formulation blends predicted that all the components would remain stable and no degradation of the drugs and excipients was likely to occur at the printing temperatures (40 °C). HPLC analysis was also used to confirm stability of amlodipine and lisinopril post-printing, with the HPLC trace showing only evidence of the main APIs peaks after sintering.

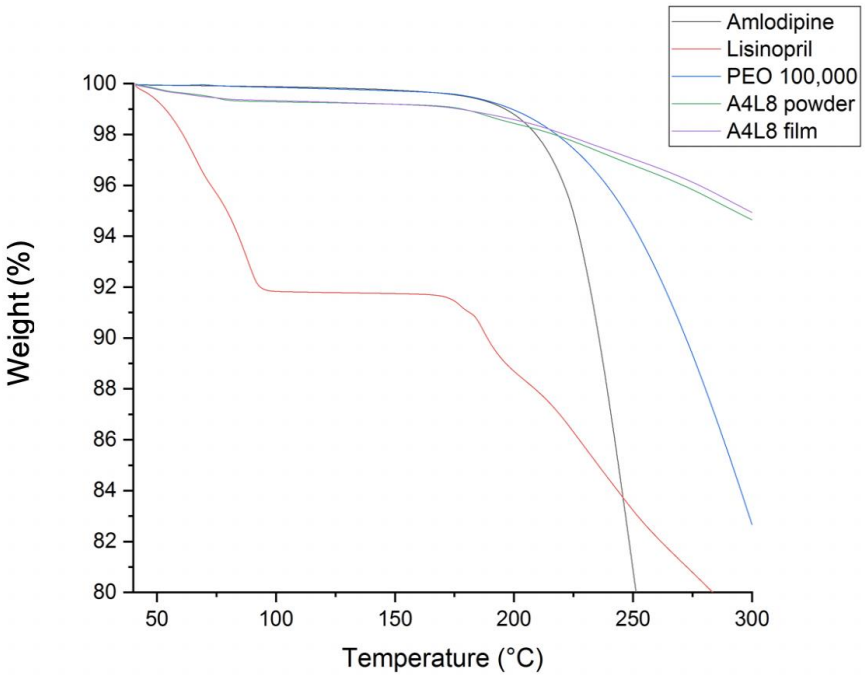

Figure 2. Thermogravimetric analysis of amlodipine, lisinopril, PEO 100,00, A4L8 formulation blend and A4L8 film.

XRPD analysis of the drug, polymers, formulation blends and printlets were performed to determine the physical state of the drugs and the degree of incorporation within the polymers (Figure 3). Characteristic patterns from the XRPD focused between 3 to 16° 2θ showed that the lisinopril drug peak present

at about 7.5° 2θ was also present in the powder blend. However, in the films, the peak became broader and showed a significant reduction in peak height. This indicates that lisinopril had been converted partially into the amorphous phase. Characteristic amlodipine peaks were present at 10° and 12° 2θ in the powder formulation but not the printed film indicating that either there was a complete conversion to the amorphous state or, alternatively, the remaining crystalline content was below the sensitivity of the XRPD method. Consistent drug and polymer peak shifts of ~+1° 2θ was apparent in the printed formulation, which was attributed to the stress–strain influence or the change in height presentation of a printed disc versus the raw powder. Such peak shifts have been observed in previous studies (Robles-Martinez et al., 2019).

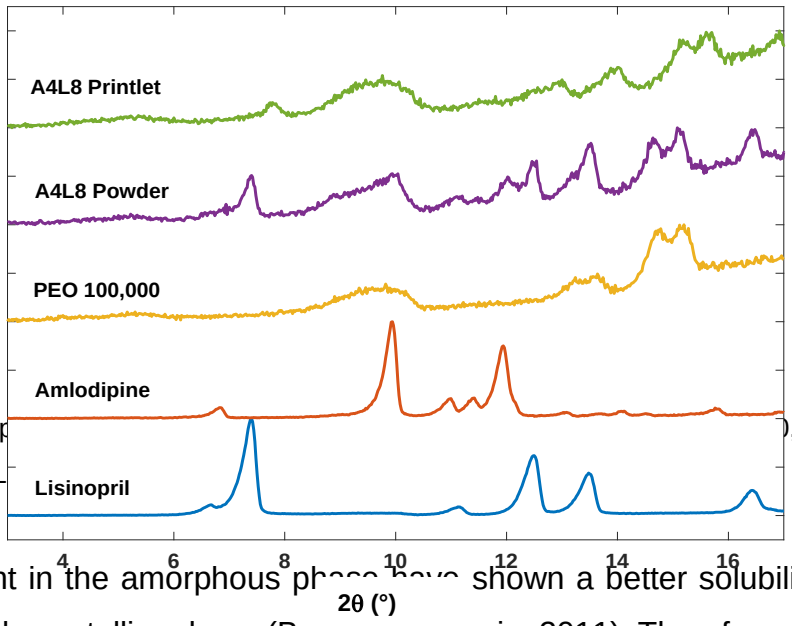

Figure 3. X-ray p),000, A4L8 powder and A4L

Drugs present in the amorphous phase have shown a better solubility profile compared with crystalline drugs (Babu and Nangia, 2011). Therefore, there are a number of advantages of delivering drugs in an amorphous form especially for drugs under BCS Class II or IV that has low solubility to enhance its dissolution and bioavailability (Capretto et al., 2017; Martinez et al., 2014). Several papers have shown the feasibility of using 3D printing technologies to formulate drugs in amorphous or semi-amorphous states to achieve enhanced drug release profiles (Goyanes et al., 2019a; Kollamaram et al., 2018; Sadia et al., 2016). During the SLS process used here, the application of the laser may

lead to complete drug melting to enable formation of the non-crystalline matrices (Trenfield et al., 2018b). However, this process will vary based on the drugs, excipients and printing parameters used, such as laser scanning speed and chamber temperature. It is worth mentioning however, that despite the benefits of formulating drugs in the amorphous phase, there could also be a risk of conversion back to its crystalline state and hence in the future accelerated stability studies are required to determine shelf life of the 3D printed drug products.

Printlet hardness was evaluated to determine the ease of handling of the developed formulations. For all the cylindrical printlets, the hardness exceeded the maximum value that the equipment could measure because the printlets did not break but they were physically deformed (Table 2). Friability of all the formulations of cylindrical printlets were less than 1%, complying with the British Pharmacopoeia (BP) requirements for uncoated tablets, making them suitable for handling and packing (BP, 2018). Favourably, percentage recoveries of both amlodipine and lisinopril were determined using HPLC, and were all found to be between the 85-115% limits that have been set by BP for content uniformity testing (Table 2). All dosage forms were found to pass weight variation tests according to the BP (<7.5% variation).

Table 2. Physical properties and recovery of the cylindrical printlets

Formulation	Weight (mg) ± SD	Crushing strength (N) ± SD	Friability (%) ± SD	Amlodipine recovery (%)	Lisinopril recovery (%)
A2L4	170.5±1.08	>483.7±0.58	0.23±0.05	103.9±4.7	96.9±0.7
A3L6	168.6±5.71	>484.0±0.00	0.57±0.48	99.1± 7.4	99.9±0.3
A4L8	163.6±3.65	>483.7±0.58	0.93±0.90	103.1±2.4	98.7±7.6

3.2. Quantitative analysis using NIR spectroscopy

In order to facilitate the integration of 3D printing for the production of antihypertensive polyprintlets at the point-of-care, a non-destructive method is required to enable at-line quality control and batch release. Previously, we have proven the feasibility of using process analytical technologies (PAT) to quantify a single model drug (paracetamol) in SLS printlets (Trenfield et al., 2018b). Here, we have investigated the use of a portable NIR spectrometer to quantify both therapeutically-relevant dosages of amlodipine and lisinopril in 3D printed oral films and cylindrical tablets. Initially, the pure drugs (amlodipine and lisinopril) and pure PEO 100,000 were scanned to identify unique peaks of interest for calibration model development (Figure 4). For amlodipine, the wavelengths selected ranged between 1450-1600 nm and 2000-2100 nm, whereas for lisinopril the wavelength selected was between 1600-1730 nm. Lisinopril also displayed a high absorbance at ~1920nm, however this peak is attributed to the presence of water due to the drug being in the dihydrate form; as such, this peak was excluded for model development. The feasibility of using the selected absorbance peaks was evaluated by scanning formulation blends of increasing drug concentrations (amlodipine: 1-4% *w/w* and lisinopril 2-8% *w/w*) (Figure 5). The NIR absorbance was found to increase upon increasing concentrations of both amlodipine (Figures 5A and B) and lisinopril (Figure 5C) formulations, indicating their suitability for calibration model development.

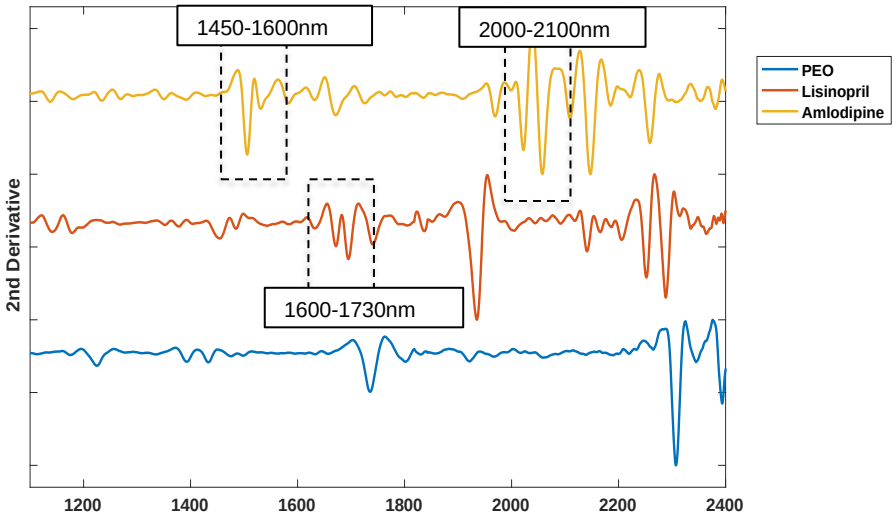

Figure 4. Second derivative spectra of PEO 100,000, lisinopril and amlodipine. Spectral features of interest were 1450-1600 nm and 2000-2100 nm for amlodipine, and 1600-1730 nm for lisinopril.

Data pre-treatment is essential to eliminate or minimise variability unrelated to the property of interest and to minimise physical effects prior to multivariate calibration, to ensure the development of an effective model (Huang et al., 2010). Pre-treatment improves the accuracy of quantification by enhancing spectral information and reducing baseline drift (Chalus et al., 2005). Evaluation of a variety of pre-processing methods was performed to create a reliable multivariate calibration model (data not shown). In this study, for amlodipine, the model selected has 4 latent variables (LVs), covers between 1450-1600 nm and 2000-2100 nm wavelength range with a second derivative (Savitzky and Golay method: filter width of 21 with a second polynomial (Savitzky and Golay, 1964)), followed by multiplicative scatter correction (MSC) and mean centering pre-processing techniques.

382

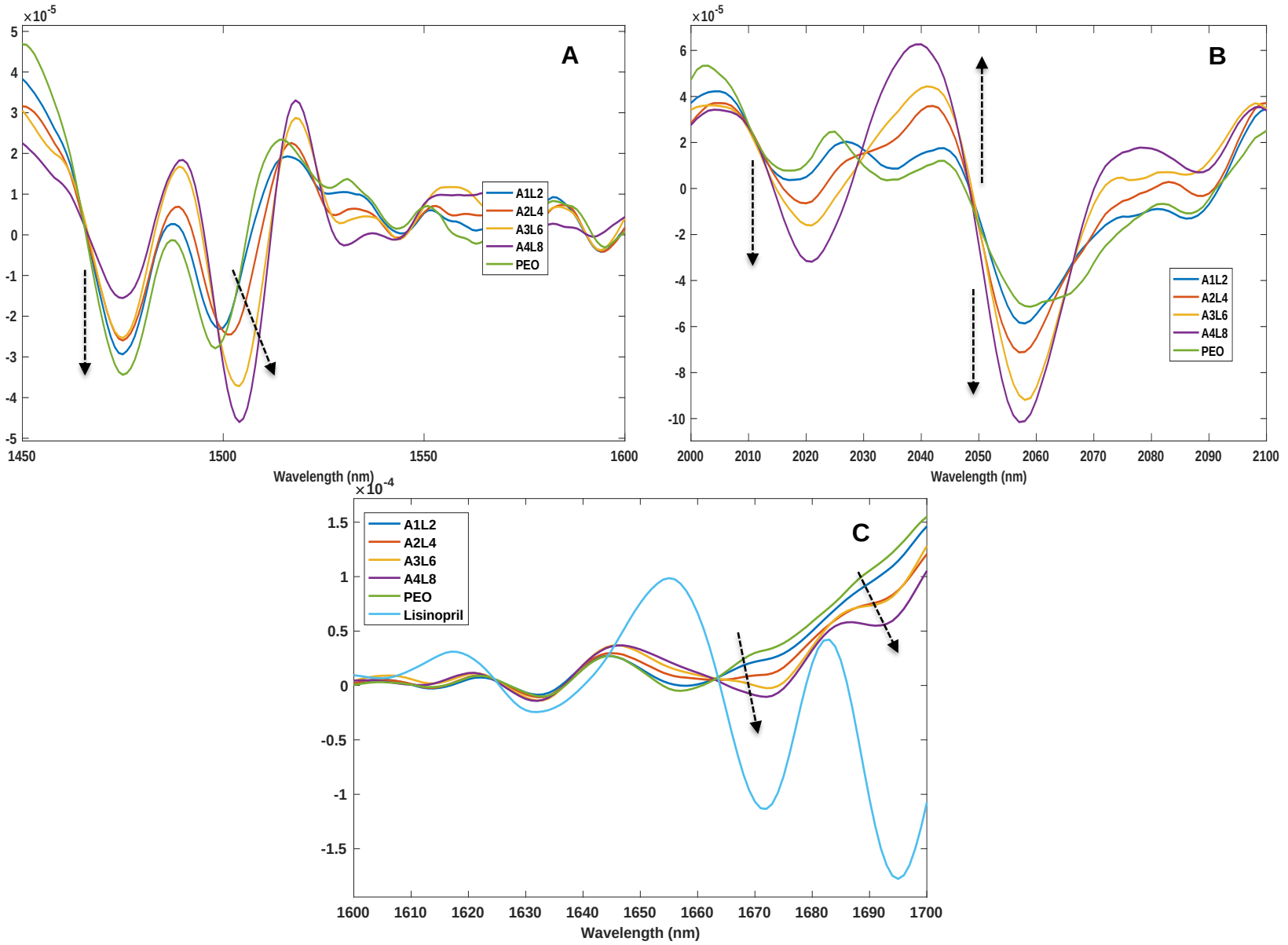
A
B
C
×10^-5
×10^-4
A1L2
A2L4
A3L6
A4L8
PEO
Lisinopril
Wavelength (nm)

Figure 5. Change in second derivative NIR absorbances with the concentration of amlodipine in A) 1450-1600 nm, B) 2000-2100 nm and lisinopril in C) 1600-1700 nm.

For lisinopril, the model selected had 4 LVs, and covers a wavelength range between 1600-1730 nm with a second derivative (Savitzky and Golay method: filter width of 15 with a second polynomial (Savitzky and Golay, 1964)), followed by standard normal variant (SNV) and mean centering pre-processing techniques. These models were selected due to having a high linearity (R^2 = 0.997 for amlodipine; 0.991 for lisinopril) and high accuracy (RMSEP = 0.24% for amlodipine; 0.24% for lisinopril) (Figures 6A and B). These values confirmed that the NIR test results were proportional to the amlodipine and lisinopril concentrations in the stated range. There are several parameters including model linearity, specificity and accuracy that are recommended by ICH (ICH, 1994a), EMA (EMA, 2014a) and FDA (FDA, 2015b) guidelines that the developed models need to satisfy to be validated.

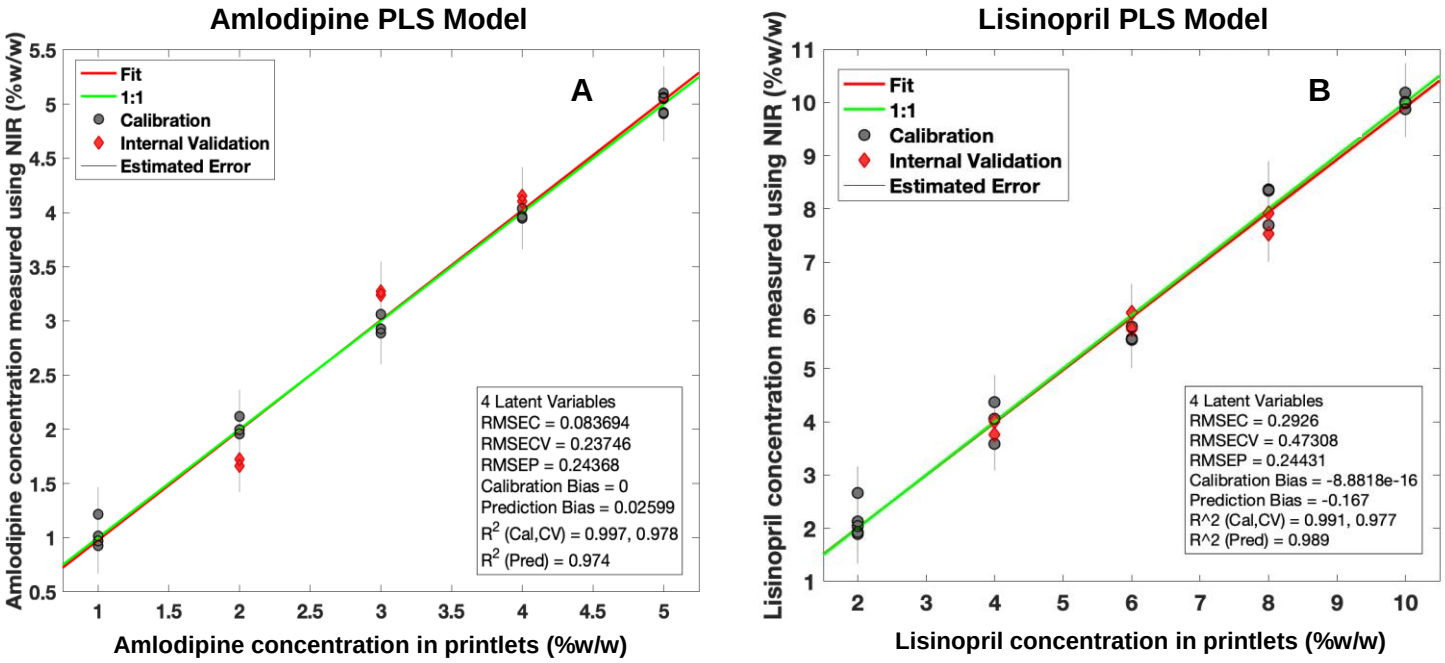

Figure 6. PLS calibration models of NIR predicted drug content (%w/w) of oral film printlets for A) Amlodipine and B) Lisinopril. Grey points are calibration (19 points from 5 concentrations); Red points are internal validation (6 points from 3 concentrations).

3.2.1 Specificity

Specificity is defined as the ability to identify definitely the analyte (amlodipine and lisinopril) from the other excipients (Candurin Gold Sheen and PEO 100,000) (Patel et al., 2012). This was evaluated by comparing the loadings spectra of the 1st latent variable (LV 1) to the pure material reference spectra, which accounted for variation of 82.77% and 79.55% for amlodipine and lisinopril, respectively (Figure 7). The LV1 spectrum was found to model well-known amlodipine spectral features at 1450-1600 nm and 2000-2100 nm (demonstrated in Figures 7A and C) and well-known lisinopril spectral features at 1600-1730 nm (highlighted in Figures 7B and D). The LV1 spectra of both amlodipine and lisinopril models were not found to be modelling common spectral features of PEO 100,0 00 (Figure 4).

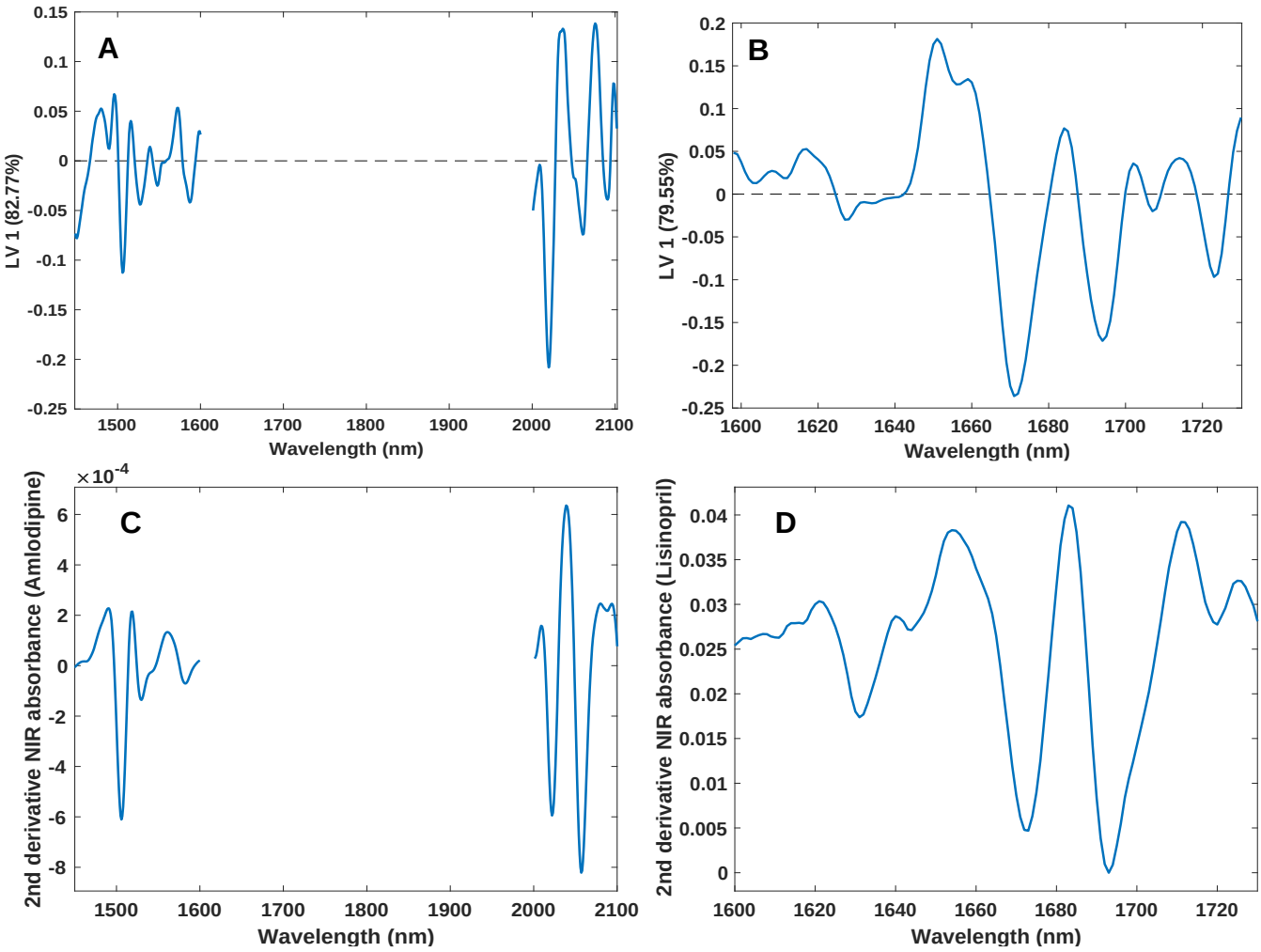

Figure 7. NIR absorbance spectra of A) Amlodipine PLS model LV1 loading spectra, B) Lisinopril PLS model LV1 loading spectra, C) Amlodipine pure and D) Lisinopril pure

3.2.2 Accuracy

The accuracy of a calibration model can be defined as the closeness in the agreement between the actual and the predicted NIR values (ICH, 1994a). As such, oral film printlets from 3 concentration levels (A2L4, A3L6 and A4L8) were scanned and the model was evaluated for prediction accuracy. An excellent predictive performance was observed with both drugs as the RMSEP for amlodipine was 0.24% and RMSEP was 0.24% for lisinopril (Figures 6A and B). Table 3 shows the difference between the HPLC and NIR predicted amlodipine and lisinopril concentrations. Paired t-test results showed that there were no significant differences between HPLC and NIR predictions as $p > 0.05$ across all three concentrations. This confirmed that NIR is a suitable quantification method for standard printlets. NIR prediction showed a higher SD compared to HPLC, which may be due to the minute differences in the surface effects of the printlets (Trenfield et al., 2018b). Generally, the model maintained a good predictive performance due to a majority of the data variation being attributed to the changes in the drugs' concentration (LV1 for amlodipine = 82.77%; LV1 for lisinopril = 79.55%).

Table 3. Results of dose predicted from oral film printlets test set using the NIR model vs the reference HPLC method

Formulation	**Test Validation**					
	Amlodipine (% *w/w*)			**Lisinopril (% *w/w*)**		
	HPLC	**NIR**	**P value**	**HPLC**	**NIR**	**P value**
A2L4	2.08±0.001	1.99±0.09	0.23	2.90±0.0001	3.03±0.27	0.54
A3L6	2.97±0.002	2.62±0.12	0.10	5.99±0.0001	5.72±0.25	0.26
A4L8	4.13±0.000	3.73±0.31	0.15	7.90 ±0.006	7.46±0.46	0.41

One of the main benefits of 3D printing for personalised medicine is the ability to tailor solid dosage form shape and size, depending on the patient preference or therapeutic needs (Trenfield et al., 2018a). Several studies have already shown that changing printlet geometry can alter the dose and drug release characteristics (Goyanes et al., 2015b; Martinez et al., 2018; Sadia et al.,

2018a). It is also well known that NIR absorbance can be affected by surface effects (Jamrógiewicz, 2012; Saeed et al., 2009) and, as such, it was important to evaluate the performance of the developed PLS model when scanning printlets of different geometries.

To determine this, cylindrical shaped printlets (amlodipine 2-4% *w/w* and lisinopril 4-8% *w/w*) with the same formulation compositions as the oral films were 3D printed and scanned using NIR at six different points on the dosage form. Figures 8A and 8B show that the model predicted the concentrations well, as the points fitted on the calibration curve. For amlodipine prediction, the change in printlet geometry from a thin film to cylindrical tablet caused a slightly higher error compared to oral films (RMSEP values of 0.26% and 0.24%, respectively). A similar occurrence observed with the prediction of lisinopril, with RMSEP values of 0.77% and 0.24% for cylindrical tablets and oral films, respectively. This phenomenon is likely due to the complex rounded surface structure of this shape compared with the flat films. However, overall the model continued to be fit-for-purpose for use with differently shaped tablets of the same composition.

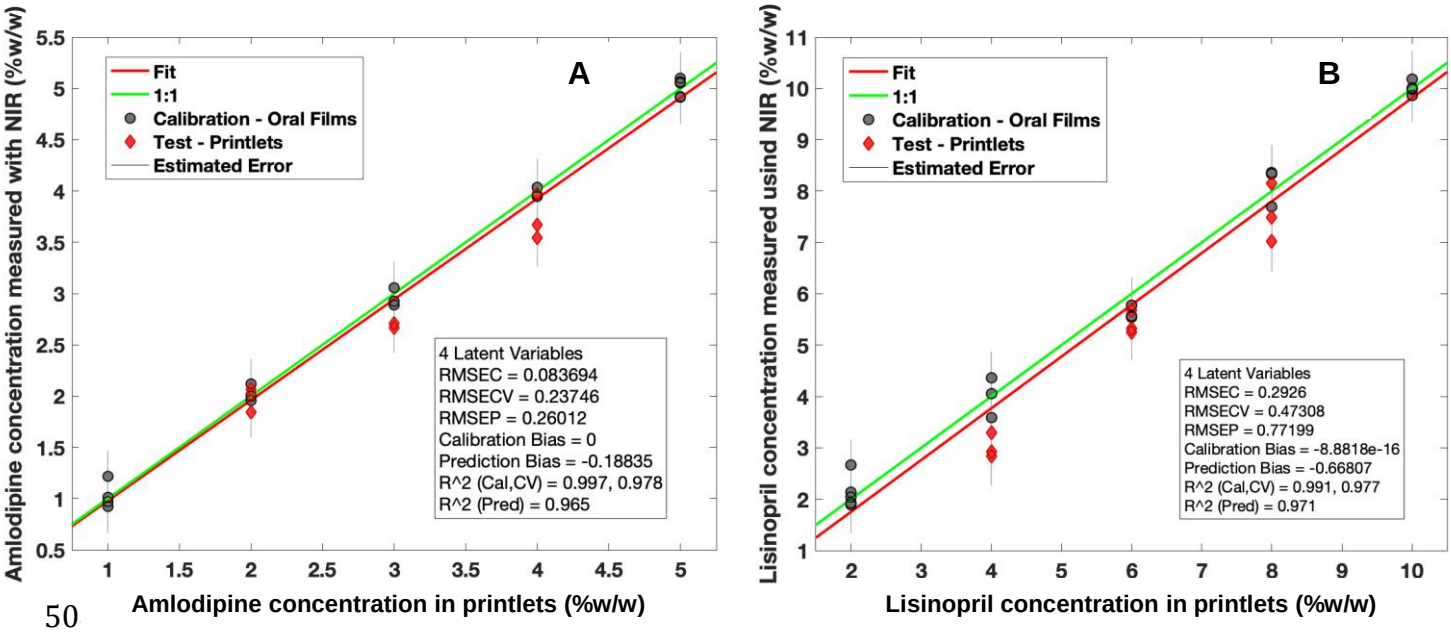

Figure 8. Application of developed PLS models of NIR predicted drug content of A) amlodipine and B) lisinopril. Grey points are calibration (based on oral films); red points are a test set of cylindrical printlets.

Currently, PLS regression is widely used for a full quantitative characterisation as it gives the highly accurate predictions (Ravn et al., 2008; Roggo et al., 2007). The non-destructive, at-line QC method demonstrated here clearly shows a lot of advantages as it is highly user-friendly and provides rapid dose prediction with the scanning time for each tablet is only roughly 10 seconds. Since the FDA and EMA guidance also recognise the use of PLS regression as a quantitative tool, the developed model in the present study is suitable to be used for quality control purposes in the clinic (EMA, 2014a; FDA, 2015b). The validation of the developed PLS models have proven the feasibility of the use of NIR spectroscopy to replace conventional destructive dose verification methods (such as HPLC and UV spectroscopy).

4. Conclusion

For the first time, we report the at-line dose verification of two separate drugs (amlodipine and lisinopril) within 3D printed antihypertensive polyprintlets. Calibration models were developed across therapeutically relevant dosages of two drugs (amlodipine: 1-5% w/w, and lisinopril 2-10% w/w) and were applicable to polyprintlets of different geometries (oral films and cylindrical tablets). The developed models demonstrated excellent linearity (R^2 pred = 0.997, 0.991), accuracy (RMSEP = 0.24%, 0.24%) and specificity (LV1 = 82.77%, 79.55%) for both amlodipine and lisinopril respectively, and were validated according to current international standards. This manuscript provides a novel method for the dual quantification of two drugs, facilitating the integration of 3D printing into clinical practice.

5. Acknowledgements

The authors thank the Engineering and Physical Sciences Research Council (EPSRC), UK for their financial support (EP/L01646X).

6. References

Abegaz, T.M., Shehab, A., Gebreyohannes, E.A., Bhagavathula, A.S., Elnour, A.A., 2017. Nonadherence to antihypertensive drugs: A systematic review and meta-analysis. Medicine 96, e5641.

Alhnan, M.A., Okwuosa, T.C., Sadia, M., Wan, K.W., Ahmed, W., Arafat, B., 2016. Emergence of 3D Printed Dosage Forms: Opportunities and Challenges. Pharm Res 33, 1817-1832.

Alomari, M., Vuddanda, P.R., Trenfield, S.J., Dodoo, C.C., Velaga, S., Basit, A.W., Gaisford, S., 2018. Printing T3 and T4 oral drug combinations as a novel strategy for hypothyroidism. International Journal of Pharmaceutics 549, 363-369.

Awad, A., Fina, F., Trenfield, S.J., Patel, P., Goyanes, A., Gaisford, S., Basit, A.W., 2019. 3D Printed Pellets (Miniprintlets): A Novel, Multi-Drug, Controlled Release Platform Technology. Pharmaceutics 11(4), 148.

Awad, A., Trenfield, S.J., Gaisford, S., Basit, A.W., 2018a. 3D printed medicines: A new branch of digital healthcare. Int J Pharm 548, 586-596.

Awad, A., Trenfield, S.J., Goyanes, A., Gaisford, S., Basit, A.W., 2018b. Reshaping drug development using 3D printing. Drug Discovery Today 23, 1547-1555.

Babu, N.J., Nangia, A., 2011. Solubility Advantage of Amorphous Drugs and Pharmaceutical Cocrystals.

Barakh Ali, S.F., Mohamed, E.M., Ozkan, T., Kuttolamadom, M.A., Khan, M.A., Asadi, A., Rahman, Z., 2019. Understanding the effects of formulation and process variables on the printlets quality manufactured by selective laser sintering 3D printing. Int J Pharm 570, 118651.

Barnatt, C., 2013. 3D Printing: The Next Industrial Revolution.

Basit, A., Gaisford, S., 2018. 3D Printing of Pharmaceuticals. DOI: https://doi.org/10.1007/978-3-319-90755-0. Springer.

BP, 2018. Appendix XVII G. Friability - British Pharmacopoeia.

Capretto, L., Byrne, G.T., S, L, D., 2017. Formulation, Analytical, and Regulatory Strategies for First-in-Human Clinical Trials, in: E, K. (Ed.), Oral Formulation Roadmap from Early Drug Discovery to Development.

578 Chalus, P., Roggo, Y., Walte, r.S., Ulmschneider, M., 2005. Near-infrared
579 determination of active substance content in intact low-dosage tablets. -
580 Abstract - Europe PMC.
581 Corrêa, N.B., de Faria, A.P., Ritter, A.M.V., Sabbatini, A.R., Almeida, A.,
582 Brunelli, V., Calhoun, D.A., Moreno, H., Modolo, R., 2016. A practical
583 approach for measurement of antihypertensive medication adherence in
584 patients with resistant hypertension. Journal of the American Society of
585 Hypertension 10, 510-516.e511.
586 Di Prima, M., Coburn, J., Hwang, D., Kelly, J., Khairuzzaman, A., Ricles, L.,
587 2016. Additively manufactured medical products – the FDA perspective |
588 SpringerLink.
589 DrugBank, Lisinopril dihydrate.
590 Durden, M., Avery, T., Rupert, P., 2013. Polypharmacy and medicines
591 optimisation. @TheKingsFund.
592 Edinger, M., Iftimi, L.-D., Markl, D., Al-Sharabi, M., Bar-Shalom, D., Rantanen,
593 J., Genina, N., 2019. Quantification of Inkjet-Printed Pharmaceuticals on
594 Porous Substrates Using Raman Spectroscopy and Near-Infrared
595 Spectroscopy. AAPS PharmSciTech 20, 207.
596 Edinger, M., Jacobsen, J., Bar-Shalom, D., Rantanen, J., Genina, N., 2018.
597 Analytical aspects of printed oral dosage forms. International Journal of
598 Pharmaceutics 553, 97-108.
599 EMA, 2012. Guideline on Real Time Release Testing (formerly Guideline on
600 Parametric Release).
601 EMA, 2014a. Use of near infrared spectroscopy (NIRS) by the pharmaceutical
602 industry and the data requirements for new submissions and variations |
603 European Medicines Agency.
604 EMA, E.M.A., 2014b. Use of near infrared spectroscopy (NIRS) by the
605 pharmaceutical industry and the data requirements for new submissions and
606 variations. European Medicines Agency.
607 FDA, 2015a. Development and Submission of Near Infrared Analytical
608 Procedures; Draft Guidance for Industry; Availability.
609 FDA, 2015b. Development and Submission of Near Infrared Analytical
610 Procedures; Draft Guidance for Industry; Availability.

611 Fina, F., Goyanes, A., Gaisford, S., Basit, A.W., 2017. Selective laser
612 sintering (SLS) 3D printing of medicines. Int J Pharm 529, 285-293.
613 Fina, F., Goyanes, A., Madla, C.M., Awad, A., Trenfield, S.J., Kuek, J.M.,
614 Patel, P., Gaisford, S., Basit, A.W., 2018a. 3D printing of drug-loaded gyroid
615 lattices using selective laser sintering. International journal of pharmaceutics
616 547, 44-52.
617 Fina, F., Madla, C.M., Goyanes, A., Zhang, J., Gaisford, S., Basit, A.W.,
618 2018b. Fabricating 3D printed orally disintegrating printlets using selective
619 laser sintering. Int J Pharm 541, 101-107.
620 Florence, A.T., Lee, V.H., 2011. Personalised medicines: more tailored drugs,
621 more tailored delivery. Int J Pharm 415, 29-33.
622 Genina, N., Boetker, J.P., Colombo, S., Harmankaya, N., Rantanen, J., Bohr,
623 A., 2017. Anti-tuberculosis drug combination for controlled oral delivery using
624 3D printed compartmental dosage forms: From drug product design to in vivo
625 testing. Journal of Controlled Release 268, 40-48.
626 Gioumouxouzis, C.I., Baklavaridis, A., Katsamenis, O.L., Markopoulou, C.K.,
627 Bouropoulos, N., Tzetzis, D., Fatouros, D.G., 2018. A 3D printed bilayer oral
628 solid dosage form combining metformin for prolonged and glimepiride for
629 immediate drug delivery. Eur J Pharm Sci 120, 40-52.
630 Goyanes, A., Allahham, N., Trenfield, S.J., Stoyanov, E., Gaisford, S., Basit,
631 A.W., 2019a. Direct powder extrusion 3D printing: Fabrication of drug
632 products using a novel single-step process. International Journal of
633 Pharmaceutics 567, 118471.
634 Goyanes, A., Buanz, A.B.M., Hatton, G.B., Gaisford, S., Basit, A.W., 2015a.
635 3D printing of modified-release aminosalicylate (4-ASA and 5-ASA) tablets.
636 European Journal of Pharmaceutics and Biopharmaceutics 89, 157-162.
637 Goyanes, A., Madla, C.M., Umerji, A., Duran Pineiro, G., Giraldez Montero,
638 J.M., Lamas Diaz, M.J., Gonzalez Barcia, M., Taherali, F., Sanchez-Pintos,
639 P., Couce, M.L., Gaisford, S., Basit, A.W., 2019b. Automated therapy
640 preparation of isoleucine formulations using 3D printing for the treatment of
641 MSUD: First single-centre, prospective, crossover study in patients. Int J
642 Pharm 567, 118497.

643 Goyanes, A., Robles Martinez, P., Buanz, A., Basit, A.W., Gaisford, S.,
644 2015b. Effect of geometry on drug release from 3D printed tablets.
645 International Journal of Pharmaceutics 494, 657-663.
646 Goyanes, A., Scarpa, M., Kamlow, M.-A., Gaisford, S., Basit, A., Orlu, M.,
647 2017. Patient acceptability of 3D printed medicines. International Journal of
648 Pharmaceutics 530.
649 Hamburg, M.A., Collins, F.S., 2010. The path to personalized medicine. N
650 Engl J Med 363, 301-304.
651 Herttua, K., Tabak, A.G., Martikainen, P., Vahtera, J., Kivimaki, M., 2013.
652 Adherence to antihypertensive therapy prior to the first presentation of stroke
653 in hypertensive adults: population-based study. Eur Heart J 34, 2933-2939.
654 Hinojosa-Torres, J., Aceves-Hernández, J.M., Hinojosa-Torres, J., Paz, M.,
655 Castaño, V.M., 2008. Degradation of lisinopril: A physico-chemical study.
656 Journal of Molecular Structure 886, 51-58.
657 Huang, J., Romero-Torres, S., Moshgbar, M., 2010. Practical Considerations
658 in Data Pre-treatment for NIR and Raman Spectroscopy.
659 ICH, 1994a. Validation of Analytical Procedures: Text and Methodology.
660 ICH, 1994b. Validation of Analytical Procedures: Text and Methodology, in:
661 Group, I.E.W. (Ed.), International Conference On Harmonisation Of Technical
662 Requirements For Registration Of Pharmaceuticals For Human Use, pp. 1-17.
663 Jamrógiewicz, M., 2012. Application of the near-infrared spectroscopy in the
664 pharmaceutical technology. Journal of pharmaceutical and biomedical
665 analysis 66, 1-10.
666 Khaled, S.A., Burley, J.C., Alexander, M.R., Yang, J., Roberts, C.J., 2015a.
667 3D printing of five-in-one dose combination polypill with defined immediate
668 and sustained release profiles. J Control Release 217, 308-314.
669 Khaled, S.A., Burley, J.C., Alexander, M.R., Yang, J., Roberts, C.J., 2015b.
670 3D printing of tablets containing multiple drugs with defined release profiles.
671 Int J Pharm 494, 643-650.
672 Kollamaram, G., Croker, D.M., Walker, G.M., Goyanes, A., Basit, A.W.,
673 Gaisford, S., 2018. Low temperature fused deposition modeling (FDM) 3D
674 printing of thermolabile drugs. undefined.

675 Lee, H.J., Jang, S.-I., Park, E.-C., 2017. Effect of adherence to
676 antihypertensive medication on stroke incidence in patients with hypertension:
677 a population-based retrospective cohort study. BMJ Open 7, e014486.
678 Martinez, L.M., Videa, M., Lopez-Silva, G.A., de Los Reyes, C.A., Cruz-
679 Angeles, J., Gonzalez, N., 2014. Stabilization of amorphous paracetamol
680 based systems using traditional and novel strategies. Int J Pharm 477, 294-
681 305.
682 Martinez, P.R., Goyanes, A., Basit, A.W., Gaisford, S., 2018. Influence of
683 Geometry on the Drug Release Profiles of Stereolithographic (SLA) 3D-
684 Printed Tablets. AAPS PharmSciTech. https://doi.org/10.1208/s12249-018-
685 1075-3.
686 NICE, 2011. Hypertension in adults: diagnosis and management.
687 Oblom, H., Zhang, J., Pimparade, M., Speer, I., Preis, M., Repka, M., Sandler,
688 N., 2019. 3D-Printed Isoniazid Tablets for the Treatment and Prevention of
689 Tuberculosis-Personalized Dosing and Drug Release. AAPS PharmSciTech
690 20, 52.
691 Ong, K.L., Cheung, B.M., Man, Y.B., Lau, C.P., Lam, K.S., 2007. Prevalence,
692 awareness, treatment, and control of hypertension among United States
693 adults 1999-2004. Hypertension 49, 69-75.
694 Patel, D.B., Mehta, F.A., Bhatt, K.K., 2012. Simultaneous Estimation of
695 Amlodipine Besylate and Indapamide in a Pharmaceutical Formulation by a
696 High Performance Liquid Chromatographic (RP-HPLC) Method. Sci Pharm
697 80, 581-590.
698 Pereira, B., Isreb, A., Forbes, R., Dores, F., Habashy, R., Petit, J.-B., A
699 Alhnan, M., Oga, E., 2018. 'Temporary Plasticiser': A Novel Solution to
700 Fabricate 3D Printed Patient-Centred Cardiovascular 'Polypill' Architectures.
701 European Journal of Pharmaceutics and Biopharmaceutics 135.
702 Pubchem, 2003. Amlodipine.
703 Pubchem, 2004. Ethylene glycol.
704 Pubchem, 2005. Lisinopril.
705 Ravn, C., Skibsted, E., Bro, R., 2008. Near-infrared chemical imaging (NIR-
706 CI) on pharmaceutical solid dosage forms-comparing common calibration
707 approaches. J Pharm Biomed Anal 48, 554-561.

Robles-Martinez, P., Xu, X., Trenfield, S.J., Awad, A., Goyanes, A., Telford, R., Basit, A.W., Gaisford, S., 2019. 3D Printing of a Multi-Layered Polypill Containing Six Drugs Using a Novel Stereolithographic Method. Pharmaceutics 11, 274.

Roggo, Y., Chalus, P., Maurer, L., Lema-Martinez, C., Edmond, A., Jent, N., 2007. A review of near infrared spectroscopy and chemometrics in pharmaceutical technologies. J Pharm Biomed Anal 44, 683-700.

Roy, A., Naik, N., Srinath Reddy, K., 2017. Strengths and Limitations of Using the Polypill in Cardiovascular Prevention. Current Cardiology Reports 19, 45.

Ruilope, L.M., 2011. Current challenges in the clinical management of hypertension. Nat Rev Cardiol 9, 267-275.

Sadia, M., Arafat, B., Ahmed, W., Forbes, R.T., Alhnan, M.A., 2018a. Channelled tablets: An innovative approach to accelerating drug release from 3D printed tablets. J Control Release 269, 355-363.

Sadia, M., Isreb, A., Abbadi, I., Isreb, M., Aziz, D., Selo, A., Timmins, P., Mohammed, A., 2018b. From ‘fixed dose combinations’ to ‘a dynamic dose combiner’: 3D printed bi-layer antihypertensive tablets. 484-494.

Sadia, M., Sosnicka, A., Arafat, B., Isreb, A., Ahmed, W., Kelarakis, A., Alhnan, M.A., 2016. Adaptation of pharmaceutical excipients to FDM 3D printing for the fabrication of patient-tailored immediate release tablets. Int J Pharm 513, 659-668.

Saeed, M., Saner, S., Oelichmann, J., Keller, H., Betz, G., 2009. Assessment of Diffuse Transmission Mode in Near-Infrared Quantification—Part I: The Press Effect on Low-Dose Pharmaceutical Tablets. Journal of Pharmaceutical Sciences 98, 4877-4886.

Savitzky, A., Golay, M.J.E., 1964. Smoothing and Differentiation of Data by Simplified Least Squares Procedures. Analytical Chemistry 36, 1627-1639.

Tibebu, A., Mengistu, D., Bulto, L.N., 2017. Adherence to prescribed antihypertensive medications and associated factors for hypertensive patients attending chronic follow-up units of selected public hospitals in Addis Ababa, Ethiopia, Int J Health Sci (Qassim), pp. 47-52.

Trenfield, S.J., Awad, A., Goyanes, A., Gaisford, S., Basit, A.W., 2018a. 3D Printing Pharmaceuticals: Drug Development to Frontline Care. Trends in pharmacological sciences 39, 440-451.

Trenfield, S.J., Awad, A., Madla, C.M., Hatton, G.B., Firth, J., Goyanes, A., Gaisford, S., Basit, A.W., 2019a. Shaping the future: recent advances of 3D printing in drug delivery and healthcare. Expert Opinion on Drug Delivery 16, 1081-1094.

Trenfield, S.J., Goyanes, A., Telford, R., Wilsdon, D., Rowland, M., Gaisford, S., Basit, A.W., 2018b. 3D printed drug products: Non-destructive dose verification using a rapid point-and-shoot approach. Int J Pharm 549, 283-292.

Trenfield, S.J., Xian Tan, H., Awad, A., Buanz, A., Gaisford, S., Basit, A.W., Goyanes, A., 2019b. Track-and-Trace: Novel Anti-Counterfeit Measures for 3D Printed Personalised Drug Products using Smart Material Inks. Int. J. Pharm. 567, 118443.

Vakili, H., Wickstrom, H., Desai, D., Preis, M., Sandler, N., 2017. Application of a handheld NIR spectrometer in prediction of drug content in inkjet printed orodispersible formulations containing prednisolone and levothyroxine. Int J Pharm 524, 414-423.

WHO, 2019. Raised Blood Pressure: Global Health Observatory data.

Xu, X., Robles-Martinez, P., Madla, C.M., Goyanes, A., Basit, A.W., Gaisford, S., 2020. Stereolithography (SLA) 3D printing of an antihypertensive polyprintlet: Case study of an unexpected photopolymer-drug reaction. Additive Manufacturing DOI: 10.1016/j.addma.2020.101071.